1993 NASA/ASEE SUMMER FACULTY FELLOWSHIP PROGRAM

JOHN F. KENNEDY SPACE CENTER
UNIVERSITY OF CENTRAL FLORIDA

LIGHTNING STUDIES USING LDAR AND LLP DATA

PREPARED BY: Dr. Gregory S. Forbes

ACADEMIC RANK: Associate Professor

UNIVERSITY AND DEPARTMENT: The Pennsylvania State University
Department of Meteorology

NASA/KSC

DIVISION: Communications and Instrumentation

BRANCH: Instrumentation and Measurements

NASA COLLEAGUE: Carl Lennon

DATE: August 16, 1993

CONTRACT NUMBER: University of Central Florida
NASA-NGT-60002 Supplement: 11

ACKNOWLEDGEMENTS

Participation in the NASA/ASEE Summer Faculty Fellowship Program has been an enjoyable and profesionally stimulating experience. Appreciation is extended to all those who support this program financially, and to the many individuals who made presentations or gave tours to the Faculty Fellows. The tours and presentations made the Faculty Fellows more aware of the scope and complexity of activities that take place at the Kennedy Space Center. Particular thanks are extended to Dr. E. Ramon Hosler, Co-Director of the NASA/ASEE Summer Faculty Fellowship Program, and to Kari L. Stiles, Administrative Assistant, who coordinated the program extremely well.

It was a great pleasure to work with Carl Lennon and others associated with the Lightning Detection and Ranging (LDAR) system in TE-CID-3. Carl Lennon is to be congratulated for the development of the LDAR system, which shows great capabilities in revealing the presence of electrical discharges within, and emanating from, thunderstorms. His support and encouragement of the applied research reported here is appreciated. The author benefitted from discussions with Launa Maier, who has vast knowledge of thunderstorms and their electrical processes. She helped acquire Lightning Location and Protection (LLP) data and helped the author establish computer networking within the NASA TE-CID-3 Weather Research Facility.

The author is very appreciative of the efforts of the NYMA employees who operate the LDAR system and archive its data, and for patiently dealing with many data requests and the increased computer load while the data were being processed. Steve Schaefer was particularly helpful in setting up access to the data-processing computer and in retrieving data for the studies described below. Preston Porter helped acquire real-time LLP data.

Greg Taylor and Mark Wheeler of the Applied Meteorology Unit (AMU; ENSCO) helped acquire Patrick AFB radar data for a case study using the McGill radar display system. Mike Maier of CSR and Gerry Talley of TE-CID-2 also helped provide LLP data.

The author extends his best regards to the meteorologists of the 45th Weather Squadron, detached out of Patrick AFB, USAF Space Command, who provide KSC with operational weather support from the Cape Canaveral Forecast Facility. It is hoped that the applied research begun this summer can help them in the difficult task of issuing lightning advisories.

Finally, the author acknowledges the efforts of all those involved in weather support of the space program. This includes Dr. Jack Ernst, Director of the Weather Support Office, NASA Headquarters (ME); John Madura, Chief, Weather Projects Office (TM-LLP-2); Dr. Frank Merceret, AMU Chief (TM-PCO-4); Jim Nicholson (DE-AST); the Spaceflight Meteorology Group of the National Oceanic and Atmospheric Administration at Johnson Space Center; atmospheric scientists at Marshall Space Flight Center; and many others.

ABSTRACT

This study intercompared lightning data from LDAR and LLP systems in order to learn more about the spatial relationships between thunderstorm electrical discharges aloft and lightning strikes to the surface. The ultimate goal of the study is to provide information that can be used to improve the process of real-time detection and warning of lightning by weather forecasters who issue lightning advisories. The Lightning Detection and Ranging (LDAR) System provides data on electrical discharges from thunderstorms that includes cloud-ground flashes as well as lightning aloft (within cloud, cloud-to-cloud, and sometimes emanating from cloud to clear air outside or above cloud). The Lightning Location and Protection (LLP) system detects primarily ground strikes from lightning. Thunderstorms typically produce LDAR signals aloft prior to the first ground strike, so that knowledge of preferred positions of ground strikes relative to the LDAR data pattern from a thunderstorm could allow advance estimates of enhanced ground strike threat. Studies described in the report examine the position of LLP-detected ground strikes relative to the LDAR data pattern from the thunderstorms. The report also describes other potential approaches to the use of LDAR data in the detection and forecasting of lightning ground strikes.

SUMMARY

The Lightning Detection and Ranging (LDAR) system shows great capabilities in detecting lightning within thunderstorms, and emanating from thunderstorms to ground or to clear air outside or above the clouds. Real-time displays of LDAR data -- monitored on a daily basis and compared to personal observations of cloud, thunder, and lightning conditions in the vicinity of KSC -- often revealed intriguing patterns of discharges. For example, in the late stages of thunderstorm systems, many long quasi-horizontal discharges spanned tens of kilometers along parallel paths which appeared to follow the top and bottom of the anvil cloud layer. LDAR can give insights into thunderstorm dynamics.

Thunderstorms typically produce LDAR signals aloft prior to the first ground strike, so that knowledge of preferred positions of ground strikes relative to the LDAR data pattern from a thunderstorm could allow advance estimates of enhanced ground strike threat. The average lead time in this study was 5.26 minutes. Only 19% of the storms showed a strike to ground within a minute of the first LDAR detection of the storm. Two remote sensing methods of detecting ground strikes were examined: the Lightning Location and Protection (LLP) system, which detects primarily ground strikes from lightning, and LDAR, using data points below 2.6 km.

Eighty-five percent of the LLP-detected ground strikes occurred within the boundaries of the LDAR data cluster associated with the thunderstorms, and 98% occurred within or less than 2 km beyond the storm LDAR data boundaries. Ground strikes were detected during 41% of the minutes while LDAR detected thunderstorms. Ground strikes tended to occur near the center of the LDAR-defined storm. Over 4000 LLP ground strikes and nearly two million LDAR data points were used in the study, which involved cases from June and July, 1993.

The report also describes other potential approaches to the use of LDAR data in the detection and forecasting of lightning ground strikes. These involved the clustering of LDAR data into volumes encompassing the lightning activity of a thunderstorm. For intercomparison, LDAR and LLP data were grouped together in samples of one-minute duration. The characteristics and evolutions of these "LDAR-defined storms" were examined in relation to concurrent and subsequent ground strikes. Three hundred ninety-one LDAR storms were defined in this manner, of which 169 (43%) produced ground strikes at some time during their existence. At forecast times more than 10 minutes, more than half of the ground strikes occur outside the boundaries of the current LDAR boundaries of the storm, indicating the development of new thunderstorm cells along the flanks of the existing storms. On days when thunderstorms were quasi-stationary, some preference was shown for future ground strikes along the southeast flank of the current LDAR pattern; when thunderstorms were moving, some preference was shown for future ground strikes along the rear (west-southwest) flank.

The LDAR characteristics of storms during minutes with ground strikes were compared to those without ground strikes. On average, when there were ground strikes the storms had many more LDAR events, much larger volume containing LDAR events, larger cross-sectional area containing LDAR events, a much larger vertical depth of LDAR events, a much greater number of LDAR events per unit volume, and a greater number of LDAR events per unit cross-sectional area.

Storms that produced ground strikes typically had more LDAR events than those which did not produce ground strikes. Sixty-two percent of the storms without ground strikes never had LDAR data rate greater than 50 data points per minute. Only 11% of the storms producing ground strikes had peak LDAR data generation rate that low. By contrast, 81% of the storms with ground strikes had a period of more than 150 LDAR data points per minute.

TABLE OF CONTENTS

LIST OF ILLUSTRATIONS

I. INTRODUCTION

The Kennedy Space Center (KSC) is located in one of the regions of the United States (and even the world) that encounters the most lightning stikes to ground per unit area (refs. 1,2,3). The possibility of lightning at the surface or aloft is, of course, a hazard that must be avoided during launches. On a daily basis, however, there are many operations at KSC which must be curtailed if there is a threat of a lightning strike to ground in the vicinity. The accuracy and timeliness of lightning advisories, therefore, has both safety and economic implications. The ultimate goal of the research described in this report is to provide information that can be used to improve the process of real-time detection and warning of lightning by weather forecasters who issue lightning advisories.

Prior to the development and implementation of remote sensing techniques for detection of lightning during the 1970s, weather forecasters had little ability to know in detail where lightning was occurring in regions beyond the range of eyesight. The locations of thunderstorms had to be estimated using radar -- based upon crude correlations between the intensity of precipitation and cloud electrification, or by recognizing characteristic shapes of thunderstorm clouds in satellite imagery. National networks of lightning remote sensing systems now exist (ref 4), that allow a direct knowledge of the location of lightning strikes to ground with accuracy of a few kilometers. Two special, denser networks of remote sensing equipment have been established to provide highly accurate information concerning lightning in the vicinity of KSC: the Lightning Location and Protection (LLP) system and the Lightning Detection and Ranging (LDAR) system. In addition, a Launch Pad Lightning Warning System (LPLWS) is operated to detect electric fields at the surface induced by thunderstorms or other atmospheric conditions, and a Catenary Wire Lightning Instrumentation System (CWLIS) detects electrical surges in wires at the launch pads when struck by lightning. Data from the LLP and LDAR systems were used in this study.

The LLP system (ref 5) detects lightning ground strikes through use of a network of magnetic direction finding antennae which sense electromagnetic disturbances in a broad band of frequencies triggered by lightning. Individual antennae detect a particular ground strike at different azimuth angles, and the location of the ground strike is essentially determined by finding the point of intersection of lines drawn from the antennae toward the source of the disturbance. The LLP system is approximately 90% efficient in detecting ground strikes near KSC, with position accuracy of about 1 km.

The LDAR system was developed by Carl Lennon and colleagues at KSC TE-CID-3 (ref 6). Its antennae detect lightning-induced disturbances at 66 MHz frequency. This system uses a time of arrival (TOA) approach, and extremely accurate timing through use of the Global Positioning System (GPS). The lightning-induced disturbance, travelling at the speed of electromagnetic propagation, arrives at different antennae at slightly different times. The three-dimensional position of the lightning source is determined by converting these time offsets into distance differences, and then performing a triangulation. The LDAR system began real-time operation in June, 1992.

The LDAR system can generate up to 10,000 data points per second, yielding numerous data points per lightning flash. Tests of the position accuracy of the LDAR data by Launa Maier have shown that within 10 km of the central antenna, 95% of the data points are accurate to better than 200m, and 50% are accurate to better than 100m. Figure 1-1 illustrates a sample plot of LDAR data during one minute, projected to their positions at the surface.

Because the LDAR system can detect thunderstorm electrical discharges aloft, it has the potential to allow anticipation and warning of imminent ground strikes.

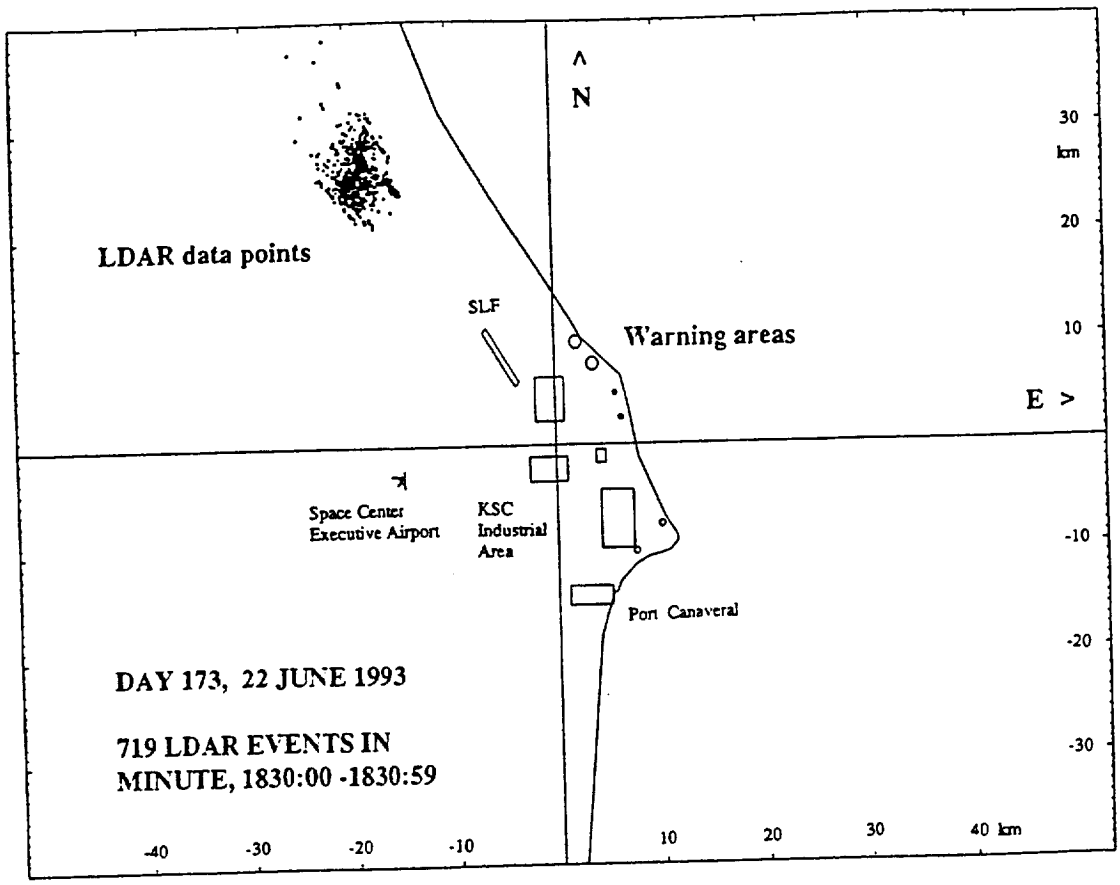

Figure 1-1. Horizontal locations of the LDAR data points that occurred on the map domain during the minute beginning at 1830 UTC on 22 June 1993 (Julian date 173), shown by dots. Circles and rectgangles represent KSC and U.S. Air Force warning areas. Solid lines cross at the LDAR central site, about 1 km north of the KSC Headquarters Building. The map domain extends 52 km west and east of the central site and 40 km north and south.

For that potential to be realized in the lightning detection and warning process, however, additional knowledge must be acquired regarding the relationship between lightning aloft and ground strikes. This project contributes to that effort.

This study examines spatial and temporal relationships between lightning aloft detected by LDAR and ground strikes detected by the LLP and LDAR systems. Several questions are addressed. (1) What is the lead time between the first detection of LDAR events and ground strikes? (2) Are there preferred locations of occurrence of ground strikes relative to the pattern of discharges detected by LDAR? (3) Can future positions of ground strikes be anticipated through knowledge of the current LDAR event pattern? (4) Are there signatures in the LDAR data that can be used to determine when the threat of ground strikes has ended? (5) Are there signatures in the LDAR data that reveal which storms produce ground strikes and which do not?

II. GENERATION OF THE DATA BASE

2.1 LDAR DATA

The time series of signals received from the LDAR network antennae are used to generate a sequential listing of LDAR data containing the x, y, and z positions of each event and the time of occurrence. The horizontal locations are given as distances east (positive x) or west and north (positive y) or south of the LDAR central site (site 0). The original data, therefore, can be used to reconstruct details of individual flashes. Data are stored in files one hour in duration.

For purposes of this study, where spatial patterns were the primary issue, the original LDAR data were converted from a data sequence into a 4-dimensional array format. Time was originally reported by day, hour, minute, second, and microsecond, and position in meters and fractions of meters. Array data in this study were accumulated in one-minute segments, and cubes 1km^3 in volume. Time accumulation was done by truncating the seconds and microseconds from the time, thereby referencing all data to the start of the minute. Horizontal accumulation was done by converting the original x, y, and z positions to integer kilometers. Finally, LDAR data points more than 52 km from the LDAR central site in the east-west direction or more than 40 km in the north-south direction were discarded. This yielded a converted data base, referred to hereafter as "LDAR cubes" or "LDAR bins", containing the number of LDAR data points per minute within each element of the array of LDAR 1 km^3 volumes. Like the original files, the LDAR cube files contain data for one hour.

The array horizontal dimensions of -52:52 by -40:40 (km) were chosen (1) to confine the study to a domain where LDAR data were highly accurate, yet (2) allow a domain sufficiently large that moving storms could be followed for at least one hour without moving out of the domain. The rectangular shape was chosen to match the aspect ratio of computer screens. The array vertical dimension was 0-20 (km), with accumulation done by integerizing the z position to the nearest kilometer. The use of 1 km vertical resolution kept the size of the data base reasonably small, but certain results below suggest that use of higher (~0.25 km) vertical resolution would have been preferable.

Figure 2-1 shows the LDAR cubes emanating from the LDAR data of Fig. 1-1. Some of the LDAR cubes overlap, suggesting the nucleus of an LDAR-defined storm classification scheme, discussed in section 2.3.

2.2 LLP DATA

The original LLP data were recorded sequentially in time and by latitude and longitude. For use in this study the time was referenced to the start of the minute, as with the LDAR data, and the horizontal position was converted to distance in kilometers east-west and north-south of the LDAR central site. LLP positions were stored as real numbers. Additional information available in the LLP data files, such as amplitude of the signal, number of return strokes per ground strike, and polarity of the lightning event, were not used in this study. Original LLP files contained all ground strikes during the day. Processed LLP data used in this study were output in hourly files to match the LDAR files.

2.3 LDAR-DEFINED STORMS

Weather forecasters use satellite imagery and weather radar to detect and track cloud and precipitation patterns, respectively. They are accustomed to identifying the patterns of satellite and radar imagery associated with rain showers

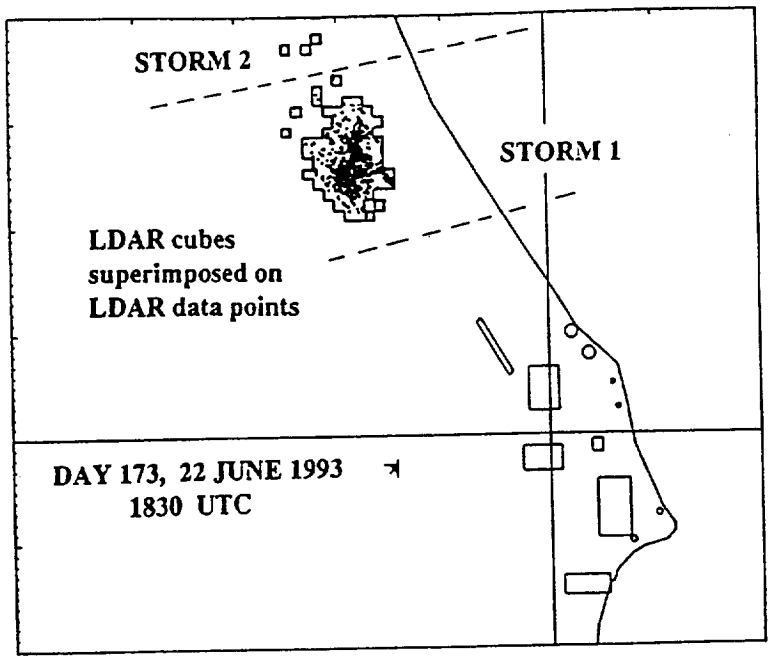

Figure 2-1. LDAR cubes superimposed on LDAR data points used in LDAR storm classification, as in Fig. 1-1, except only a portion of the domain is shown.

and thundershowers. Likewise, as can be seen from Fig. 2-1, the LDAR data points are clustered into packets affiliated with thunderstorms. It seemed natural, then, to cluster the LDAR cube data into groups, yielding "LDAR-defined storms" or "LDAR storms."

While humans can visually recognize patterns and clusterings of data readily, rules must be specified before comparable results can be obtained by computer. In the first pass of the computerized storm classification procedure, LDAR cubes from a particular minute are examined. Contiguous groupings of LDAR cubes, or near-contiguous groups within 3 km horizontal distance of each other, are clustered together to form LDAR-defined storms. The storm classification scheme proceeds by first finding the mean (x,y) position of all LDAR cubes during the minute and clustering the LDAR cubes nearest the domain mean into an LDAR storm. The storm classification scheme then continues until all LDAR cubes within the domain have been assigned a storm number. LDAR cubes separated by more than 3 km from an identified LDAR storm trigger the initiation of a new LDAR storm. For example, the closest of the three LDAR cubes farthest north on Fig. 2-1 is 4 km from the cluster of LDAR cubes to the south, so that these three will be classified as LDAR storm 2. All other LDAR cubes are within 3 km of a neighbor, and are clustered to form LDAR storm 1.

Figure 2-2 shows the result of the first pass of the LDAR storm classification scheme, from a different case. This is for minute 1800 UTC of Julian day 188, 7 July 1993. Five LDAR storms have been identified in this pass.

A second pass in the storm classification procedure eliminates "false storms" and renumbers the remaining LDAR storms consistently within the hourly file. LDAR storms were considered to be false storms if they had volume less than 4 km^3. In terms of LDAR cubes, this means that at least four LDAR cubes had to contain at least one LDAR data point during the minute. This lenient rule would not discard a true lightning event, characterized by hundreds or thousands of LDAR data points, but typically eliminates spurious points such as those generated by electrically noisy automobiles, test signals at the central site, and the occasional false LDAR point passed by the LDAR quality control procedures.

Figure 2-3 shows the result of the second pass of the LDAR storm classification scheme. In this case, false LDAR storms 2 and 5 of Fig. 2-2 have been discarded due to sub-threshold volume dimensions, and the remaining three storms have been renumbered.

Consistent LDAR storm numbering from minute to minute becomes complicated if LDAR storm shape changes dramatically or when adjacent LDAR storms expand toward each other and merge. The storm classification procedure keeps track of the horizontal position of each storm by computing the centroid position. This is the weighted-mean position of the LDAR cubes comprising the storm, where weighting is done by the number of LDAR events in the cubes. The rule invoked in the storm classification scheme is that a new storm identification number is initiated if the centroid position of the storm being processed is more than 6 km from the position of any storm during the preceeding minute. Otherwise, the storm with centroid position nearest to a storm in the preceeding minute is assigned its identification number. Should a large LDAR storm split into several LDAR storms (separated, by definition, by more than 3 km), the new storm nearest the original storm centroid would take the parent storm number and the other storms resulting from the split would obtain new storm identification numbers.

Consistent LDAR storm numbering is also complicated by the fact that in early and late stages some LDAR storms flash intermittently. During individual minutes the LDAR storm may disappear. The second pass of the storm classification procedure keeps track of the previous positions and identification numbers of all LDAR storms during the past 10 minutes. Intermittent LDAR storms that "reappear" within 10 minutes and 6 km of their previous positions retain their original numbers. In the unlikely event that a storm was inactive for more than 10 minutes, but reappears, it would be reassigned a new identification number.

In summary, after a two-pass procedure, LDAR-defined storms are numbered consistently for each minute during the hourly file. Clusters of LDAR cubes are identified as new LDAR storms when they are separated by more than 3 km from other LDAR cube clusters (storms) and when their centroid is separated by more than 6 km from any previously identified LDAR storm. This can occur (1) when isolated storms suddenly appear; (2) when an existing LDAR storm expands so dramatically and asymmetrically that its centroid shifts by more than 6 km; (3) when existing LDAR storms merge into a single, larger storm; (4) when an existing LDAR storm splits into several smaller LDAR storms; (5) when a previous LDAR storm that has been inactive for more than 10 minutes reappears. The percentage breakdown of these possibilities has not yet been studied, but it is believed that (1), (2), and (3) dominate.

The storm classification procedure generated a new three-dimensional (x,y,t) array of data containing LDAR storm identification numbers. This array identifies during each minute the LDAR storm number associated with the horizontal position x,y. If no LDAR cube in the column above point x,y contained any LDAR events during the minute, the array value was set to zero.

In the intercomparison studies of section 3, LLP ground strikes were attributed to the storm nearest to the LLP location. The nearest storm was identified by

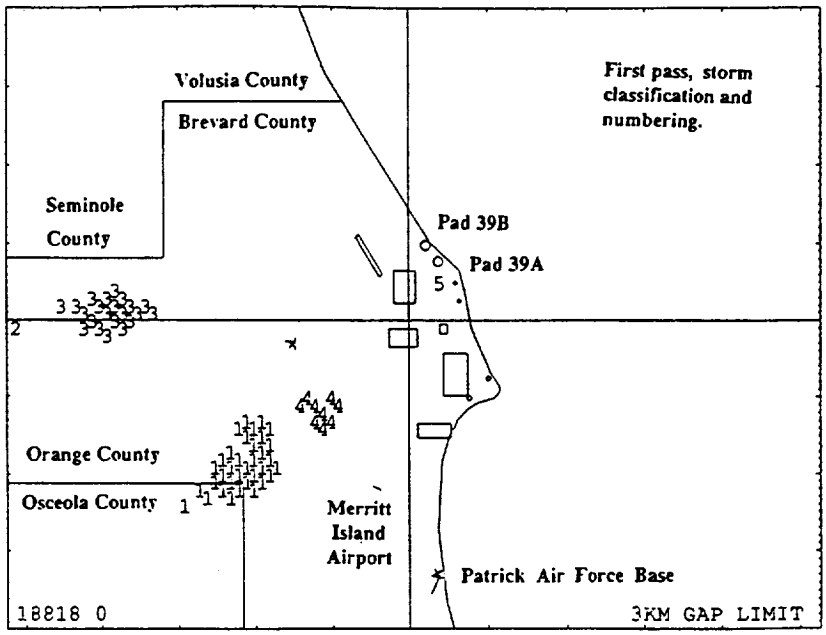

Figure 2-2. LDAR storm identification numbers resulting from the first pass of the storm identification scheme, from 1800 UTC, Day 188, 7 July 1993. A few additional landmarks have been shown.

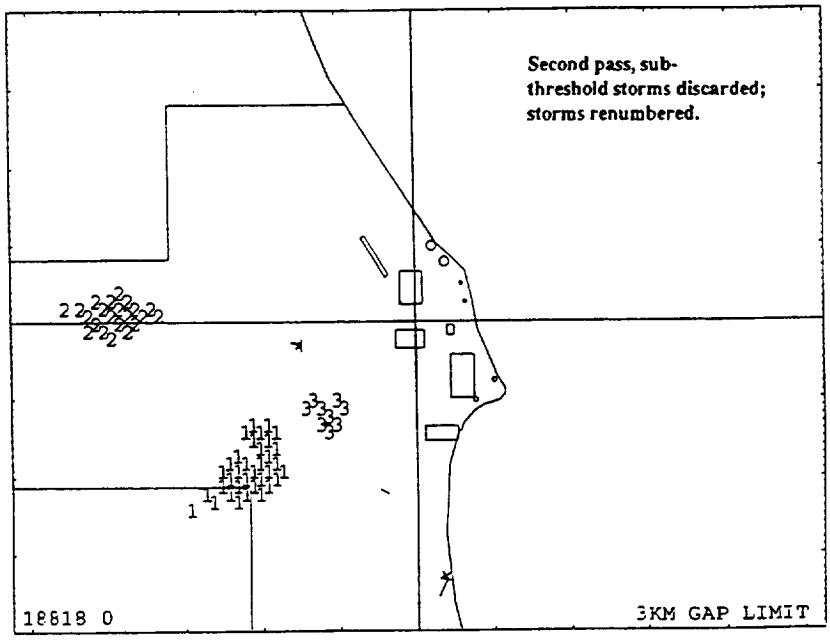

Figure 2-3. LDAR storm identification numbers after the second pass of the storm identification scheme. Identical to Fig. 2-2 except "false" storms 2 and 5 of Fig. 2-2 have been dropped and the remaining storms renumbered.

first finding the LDAR cube that contained LDAR events located nearest to the LLP data point, and then determining the LDAR storm identification number attributed to that cube.

2.4 COMPOSITE DATA BASE

The data base used in this study is the set of hours when both LDAR cube files and processed LLP files were available, and contained lightning events within the analysis domain. This consisted of 33 hours during June and July, 1993. The primary set of cases spanned the period from 22 June (day 173) to 21 July (day 201). A few additional hourly LDAR files were examined when no LLP events occurred within the map domain, but results from these have not been included in the results reported below.

The composite data base contained 1,853,170 LDAR data points and 4179 LLP ground strikes. The two-phase storm classification procedure described above identified 319 LDAR storms in this data set, of which 169 (43%) were affiliated with an LLP event during one or more minutes of their existence.

2.4.1 DERIVED LDAR PARAMETERS. During the LDAR storm classification procedure and subsequent data processing a number of additional parameters were derived from the LDAR storm and LDAR cube data base information. These included:

(1) LDAR Storm Events -- total number of LDAR data points within the LDAR storm volume;
(2) LDAR Storm Volume -- sum of the number of LDAR cubes (total km^3) containing LDAR events;
(3) LDAR Storm Area -- sum of the number of LDAR columns which contained LDAR events in some LDAR cube (essentially the LDAR storm cross-sectional area in km^2);
(4) LDAR Volume Density -- number of LDAR data points per km^3, obtained by dividing the number of LDAR Storm Events by the LDAR Storm Volume;
(5) LDAR Area Density -- number of LDAR data points per km^2, obtained by dividing the number of LDAR Storm Events by the LDAR Storm Area;
(6) LDAR Centroid X, Y, Z Positions -- weighted mean positions of the LDAR cubes comprising the LDAR storm, weighted by the number of LDAR data points within the cubes;
(7) LDAR Storm Breadth XS and YS and Depth ZS-- standard deviations of the x, y, and z positions of the LDAR cube positions comprising the storm;
(8) LDAR Storm Z95 -- height below which 95% of the LDAR data points occur in the storm;
(9) LDAR Storm Velocity Components CX, CY -- speed of LDAR storm movement in the east-west (positive when toward E) and north-south (positive when toward N) directions, based upon a least-squares fit of all storm centroid positions during the hour;
(10) LDAR Storm Duration -- number of minutes between first and last appearance of the LDAR storm;
(11) LDAR Storm Minutes -- number of minutes during which an LDAR Storm produced LDAR events (i.e., eliminating "inactive" minutes);
(12) LDAR-Based Ground Strikes -- these were obtained by identifying LDAR cubes below a threshold altitude, determined empirically, as described in Section 3.3.

Figure 2-4 shows a map of LDAR storm tracks that occurred between 1500 and 1559 UTC on 29 June 1993. This map was produced after pass 1 of the storm classification scheme, and storms 5, 7, and 9 are discarded during pass 2. LDAR storm movement tends to be somewhat wobbly, but an overall movement toward the east-southeast can be seen for storms 3 and 4. Other storms had shorter duration. The wobbly character of LDAR storm movement is due partly to quasi-

horizontal lightning flashes into new sections of cloud, causing abrupt lateral shifts in the LDAR storm centroid from one minute to the next.

Figure 2-5 shows time series of the x, y, and z centroid values as a function of time for storm 4 of Fig. 2-4. Dotted lines depict values one standard deviation above and below the mean, giving a measure of storm width in east-west and north-south directions and storm depth. Considerable growth is shown in all dimensions prior to the period of most frequent ground strikes.

Figure 2-6 shows the time variations of three other LDAR-derived parameters in relation to ground strikes: LDAR storm events, LDAR storm volume, and LDAR storm area. These are again for storm 4 of Figs. 2-4 and 2-5.

Figure 2-7 shows the time variations of three additional LDAR-derived storm parameters in relation to ground strikes for storm 4: LDAR volume density, LDAR area density, and Z95, the height below which 95% of the LDAR storm data points occur. LDAR volume density and LDAR area density appear to correlate rather well in this case with number of ground strikes per minute, with the peaks in ground strike rate occurring about 4 minutes after the peaks in volume and area density. Variations in Z95 are much more suppressed than the other parameters, and have apparently been suppressed due to use of LDAR cubes 1 km in vertical dimension. This appears to have been too coarse, and perhaps the LDAR bins should have had vertical dimension of about 0.25 km.

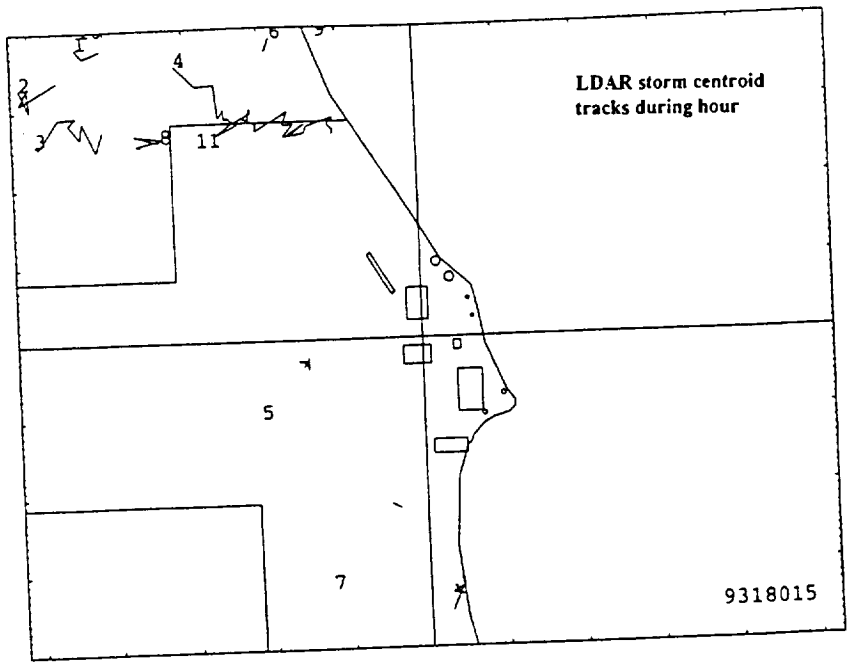

Figure 2-4. Map of LDAR storm tracks, from hour beginning 1500 UTC of day 180, 29 June 1993, after first pass of LDAR storm identification scheme.

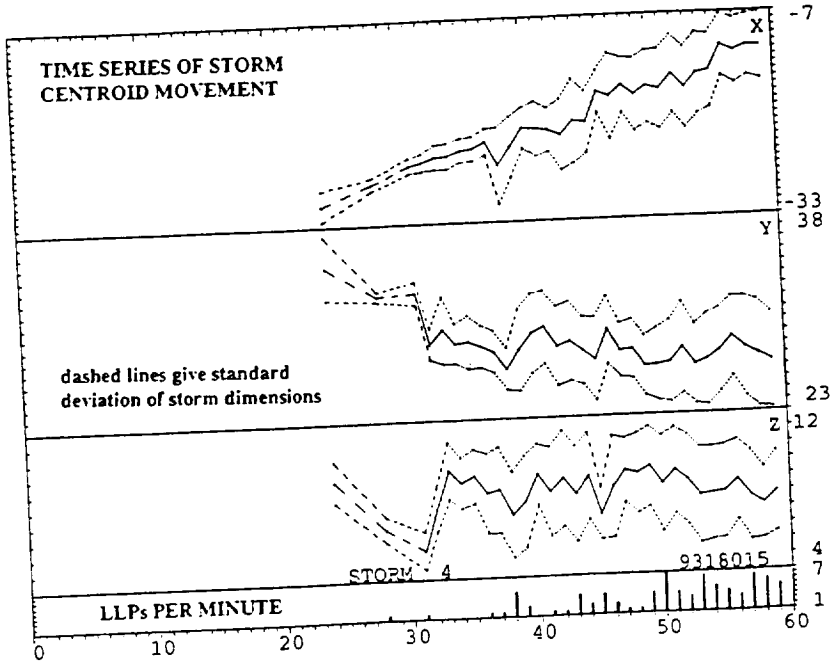

Figure 2-5. Time series of LDAR storm x, y, and z centroid positions, for storm 4 of Fig. 2-4. Number of LLP ground strikes per minute also shown.

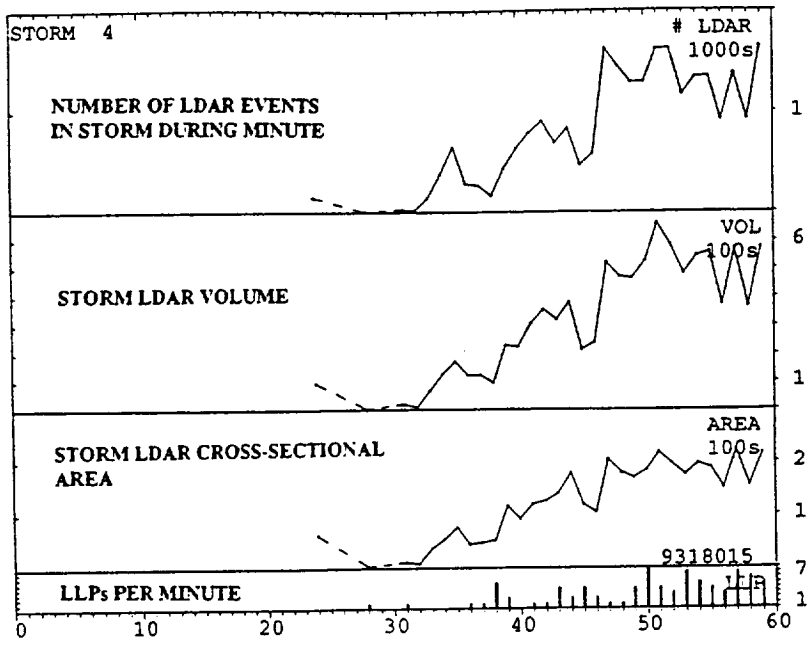

Figure 2-6. Time series of three LDAR-derived storm parameters in relation to LLP ground strikes: LDAR storm events, LDAR storm volume, LDAR storm area. For storm 4 of Figs. 2-4 and 2-5.

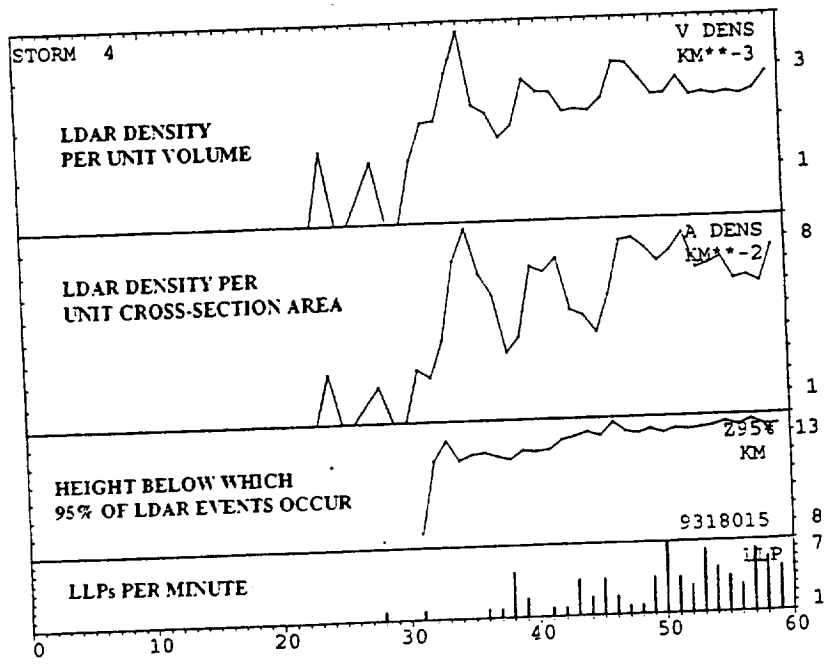

Figure 2-7. Time series of three additional LDAR-derived storm parameters in relation to LLP ground strikes: LDAR volume density, LDAR area density, and LDAR storm Z95. See text for explanations. For storm 4 of Figs. 2-4 to 2-6.

III. INTERCOMPARISON OF LDAR AND LLP DATA

3.1 LDAR LEAD TIME

Time ran out in the summer project before the author could conduct phase 3 of the storm classification project. This would have intercompared hourly files and renumbered storms consistently from one hourly file to the next. Because this phase of the project was not completed, studies of LDAR lead time used only a subset of the total data base. Eight hourly files were used, from days when these hours assuredly contained the initial formation of storms within the domain. Twenty-seven LDAR storms occurred during these hours. The average lead time between the first LDAR data defining a storm and the first LLP ground strike associated with the storm was 5.26 minutes. Only 3 of the 27 LDAR storms, 11%, had LLP ground strikes during the first minute of their existence.

Data were actually computed using all hourly files, and considering all LDAR storms in these files. Some of the first LDAR storm minutes determined in this manner will be from the first minute of the hour, though, and not really represent newly formed storms. Other first LDAR storm minutes will be from existing storms that moved into the domain. A qualitative inspection of the evolution of selected storms suggested that ground strikes were more frequent during the mature stages of storms than in the initial minutes or the late stages. Thus, LDAR storm "first minutes" in the full sample are expected to reveal a higher percentage producing ground strikes. This would also be manifested in a fictitiously low average lead time of 2.71 minutes. Of the 169 LDAR storms in the full sample, 19% of the "first" minutes had LLP ground strikes, but this number is fictitiously high.

3.2 PERCENTAGE OF TIME LDAR STORMS PRODUCE GROUND STRIKES

LDAR-defined storms were compared to ground strikes identified by LLP. Fourty-one percent of the storm-minutes were associated with LLP ground strikes. Some LDAR storms never were associated with LLP ground strikes.

3.3 LDAR DETECTION OF GROUND STRIKES

LDAR cubes centered at 0, 1, 2, and 3 km were considered as potential indicators of lightning ground strikes. The highest LDAR events in these cubes are at altitudes slightly less than 0.5, 1.5, 2.5, and 3.5 km, respectively. Table 3-1 shows the number of LDAR-based column-minutes present in the sample using various height thresholds. A column-minute is defined as a minute when any LDAR cube in the column of 1 km^2 cross-sectional area contained LDAR data points at an altitude below the threshold. Very few LDAR data points are detected below 0.5 km.

TABLE 3-1. NUMBER OF COLUMN MINUTES WITH LDAR CUBES BELOW REFERENCE ALTITUDES

Altitude	LDAR Column Minutes
1.5 km	494
2.5 km	2840
3.5 km	7801

If it is assumed that a ground strike only occurs once in an LDAR column per minute, the numbers in Table 3-1 represent the number of LDAR-deduced ground strikes using the LDAR cube data base. To match the number of ground strikes detected using the LLP system when LDAR data was available, 3190, the best threshold altitude for LDAR data is determined by interpolation to be 2.62 km.

LLP ground strikes and LDAR-estimated ground strikes, using a threshold of 2.5 km for LDAR columns, were also intercompared on an LDAR storm basis. Both LLP and LDAR systems showed ground strikes associated with the storms during 798 minutes. Both LLP and LDAR systems showed that ground strikes were absent from storms during 1174 minutes. There were 309 storm-minutes when the LLP system indicated ground strikes were present and LDAR did not. There were 318 storm-minutes when LDAR indicated ground strikes were present and LLP did not.

Case studies (and past studies of LDAR detection efficiency) suggest that the efficiency of detection of near-ground strikes may decrease with increasing distance from the LDAR central site. Thus, it would probably be most accurate to determine a threshold altitude that was a function of distance from the LDAR central site.

3.4 LOCATION OF GROUND STRIKES RELATIVE TO LDAR STORMS

Positions of ground strikes detected by LLP and LDAR systems were composited with respect to the LDAR storm centers. This was done in three ways. One compositing method counted the number of ground strikes in one-kilometer distance increments with respect to the LDAR storm center. The mean distance to the LDAR storm edge was computed along a radial from the LDAR storm centroid through the ground strike location. The drawback to this method is that individual storm widths varied greatly, making it difficult to determine the percentage of ground strikes which occurred within the LDAR storm boundary. Ground strikes were also composited by distance east/west and north/south of the LDAR storm center.

A second, "fractional" compositing method involved computing the distance to the ground strike location and the distance to the LDAR storm edge along the radial between the LDAR storm center and the ground strike location. The ground strike locations inside the LDAR storm boundary were composited by fractional distance to the storm edge, in categories 0 to 10. Category 0 included ground strikes from the LDAR storm center outward to a distance less than 5% of the way to the storm edge. Category 10 included ground strikes at a distance 95% of the distance to the storm edge outward to 5% beyond the storm edge (or to just less than 0.5 km beyond storm edge, whichever was greater). Category 5, for example, included ground strikes from 45% to just less than 55% of the distance to the storm edge. Ground strikes were also composited by fractional distance east/west and north/south of LDAR storm center. When ground strikes were outside the LDAR storm edge in this second method, they were composited in one-kilometer increments as in method 1. Category 11 included ground strikes 0.5 to just less than 1.5 km beyond LDAR storm edge and category 20 representing ground strikes 9.5 km or more LDAR beyond storm edge.

A third compositing method was used with moving LDAR storms. Here it was anticipated that there might be a preference for ground strikes in the quadrant toward which the LDAR storm was moving, for example. Thus, the third compositing method used a storm-relative frame of reference: forward/rear and left/right with respect to storm movement. Left and right orientations are determined by looking from behind the LDAR storm toward the direction it is moving. Ground strikes were then composited by distances and by fractional positions forward/rear and left/right of the LDAR storm center with respect to the storm movement vector.

Figure 3-1 shows the locations of ground strikes relative to the LDAR storm during the same minute period. This diplay is based upon the second compositing method above; i.e., by fractional distance to the LDAR storm edge, which is located at category position 10 along the x axis. Figure 3-1a depicts ground strikes detected using the LLP system; Figure 3-1b depicts LDAR ground strikes in terms of LDAR columns below 2.5 km. Eighty-five percent of the LLP ground strikes occur within the boundaries of the LDAR storm, and 98% occur either inside or within 2km beyond the edge of the LDAR storm. By definition, 100% of the LDAR-deduced ground strikes occur within the boundaries of the LDAR storm.

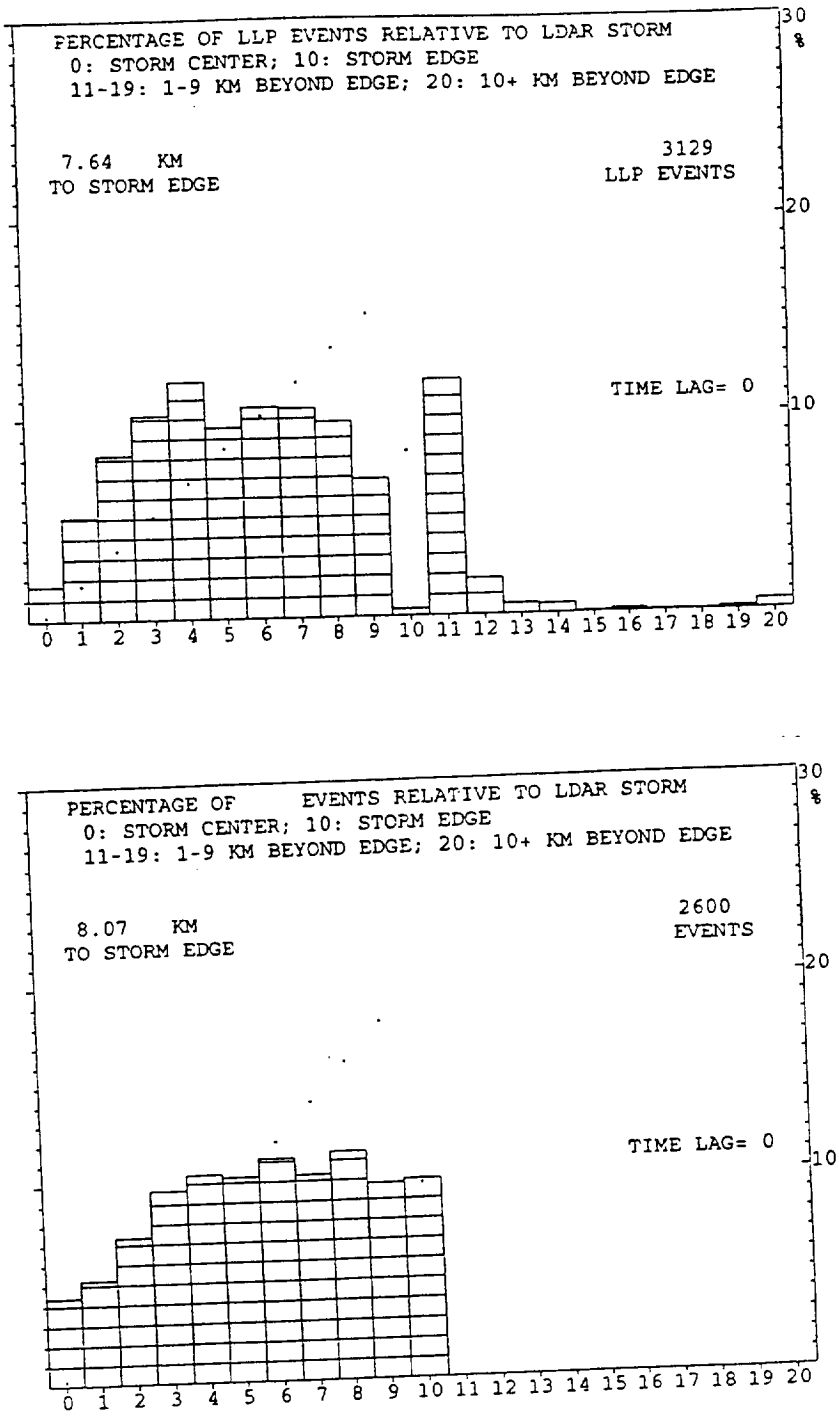

Figure 3-1. Locations of ground strikes relative to LDAR storm center, by fractional distance to edge of LDAR storm, which is at position 10.
a. (Top) LLP ground strikes.
b. (Bottom) LDAR-derived ground strikes, using LDAR data cubes below 2.5 km.

Care must be taken in interpreting Fig. 3-1. The fractional categories represent ring-shaped areas concentric about the LDAR storm center. The area within the ring increases with distance from the LDAR storm center. Thus, the area represented by small-numbered fractional categories near the LDAR storm center is small, and a small percentage of the events would be expected to occur there. For this reason, also shown on Fig. 3-1 are dots. The dots represent the percentage of ground strikes expected in the fractional categories if ground strikes were distributed in equal concentration (number per unit area) within the LDAR storm boundaries. Graphed percentages above the dots, then, indicate observed ground strike concentrations greater than average. Graphed percentages below the dots indicate observed ground strike concentrations less than average. It can be seen that the inner half of the composite LDAR storm contained greater ground strike concentrations than the outer portion.

Figure 3-2 shows the locations of ground strikes relative to the LDAR storm during the same minute period, broken down into east/west and north/south positions. Again, the dots represent expected percentages if ground strikes concentration was uniform inside the LDAR storm. The ground strikes are essentially distributed evenly on each side of the LDAR storm, with greater concentrations than average in the inner half of the composite storm.

Figure 3-3 shows the locations of ground strikes relative to the LDAR storm during the same minute period, but composited by distance from the LDAR storm center (using compositing method 1). Here the tendency for ground strikes near the LDAR storm center shows up very strongly.

3.5 SUBSEQUENT GROUND STRIKES RELATIVE TO CURRENT LDAR STORM

Weather forecasters must issue lightning advisories when ground strikes are expected within 5 nautical miles (9.25 km) of a warning site. Because they need to issue the advisories in advance of the first ground strike, it is desirable to examine the relationship of future ground strikes to the current LDAR position. Such intercomparisons have been done with time "lags" of 1, 3, 5, 10, 15, and 20 minutes.

In performing these compositings, it was anticipated that the results might be different for quasi-stationary storms and moving storms. It was also recognized that in the case of moving storms a storm-relative frame of reference would probably be most appropriate. In the latter approach, compositing method 3 of section 3.4, the movement of the LDAR storm was considered, so that the ground strike was composited with respect to the LDAR storm displaced to its future location at the time of the ground strike. The LDAR storm was presumed to remain the same size and shape during the period. In actuality, the LDAR storm-relative position of the ground strikes was obtained by displacing the ground strike points by a vector - C dt , where C is the movement vector of the LDAR storm and dt is the "time lag" (ground strike time minus current LDAR storm display time).

Table 3-2 shows the results of the time-dependent compositings for LLP ground strikes with respect to LDAR storms. For reference to the above discussion, time 0 is shown, representing intercomparison of ground strikes to LDAR storm within the same minute. The columns affiliated with "All Storms" represent an intercomparison of all storms, and the storms are presumed to remain at their current positions in their current shapes and sizes. In the columns affiliated with "Quasi-Stationary" storms, only storms whose speed could be computed and with speed of movement components less than 2.5 kts (4.6 km/h) in both the east/west and north/south directions have been composited. As in the case of "All Storms", compositing has been done with respect to the current position of the LDAR storm. There were 435 storm-minutes of this type at time 0, decreasing to 324 by time = 20 minutes (an artifact of only using hourly files). In the columns affiliated with "Moving" storms, only LDAR storms having speed of movement greater than 2.5 kts (4.6 km/h) and less than 49 kts (90.7 km/h) were composited. The setting of an upper limit discarded a few storms where the computed LDAR storm velocity was

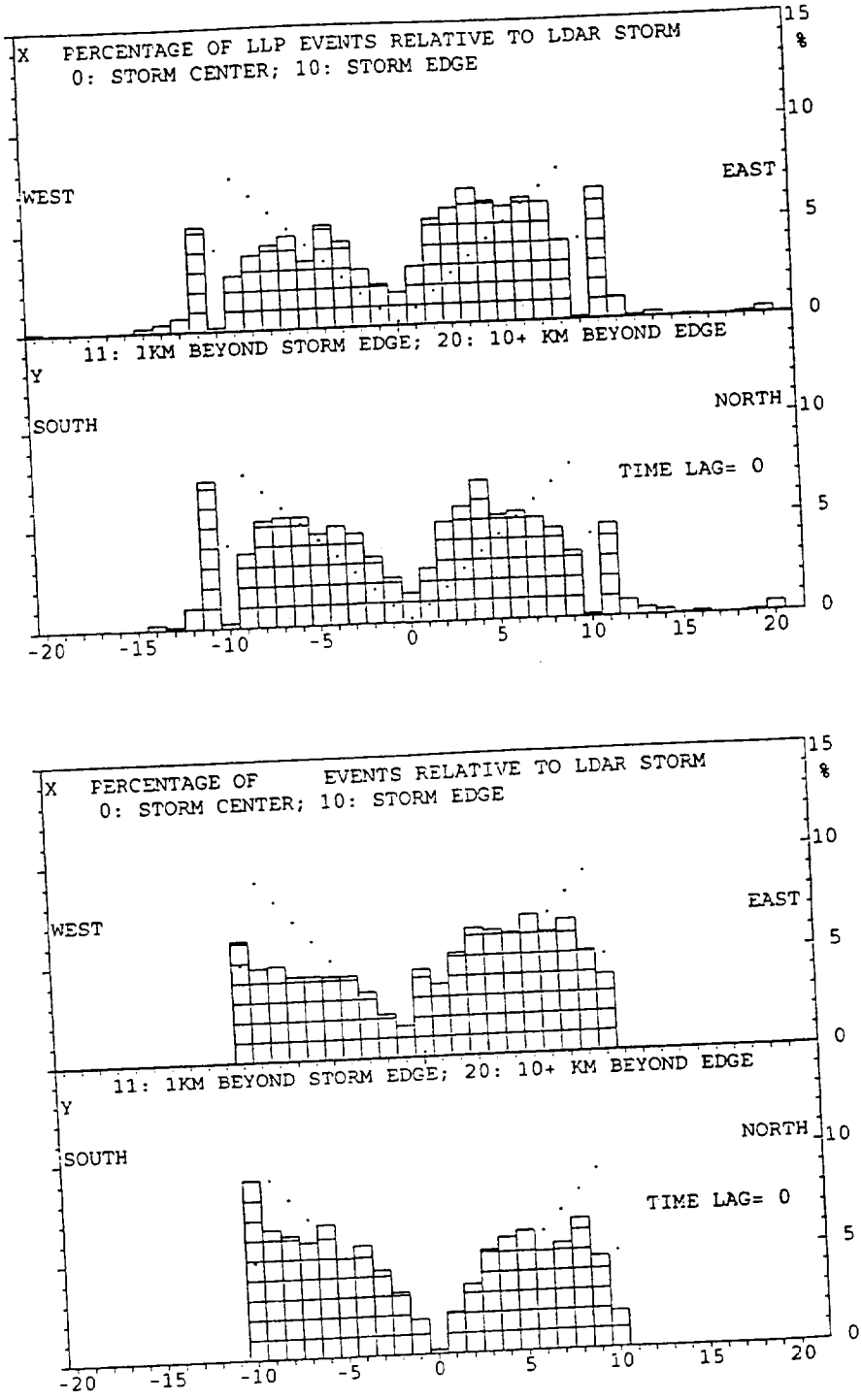

Figure 3-2. Locations of ground strikes relative to LDAR storm center, by fractional positions east/west and north/south. Edge of LDAR storm is at position 10. a. (Top) LLP ground strikes. b. (Bottom) LDAR-derived ground strikes, using LDAR data cubes below 2.5 km.

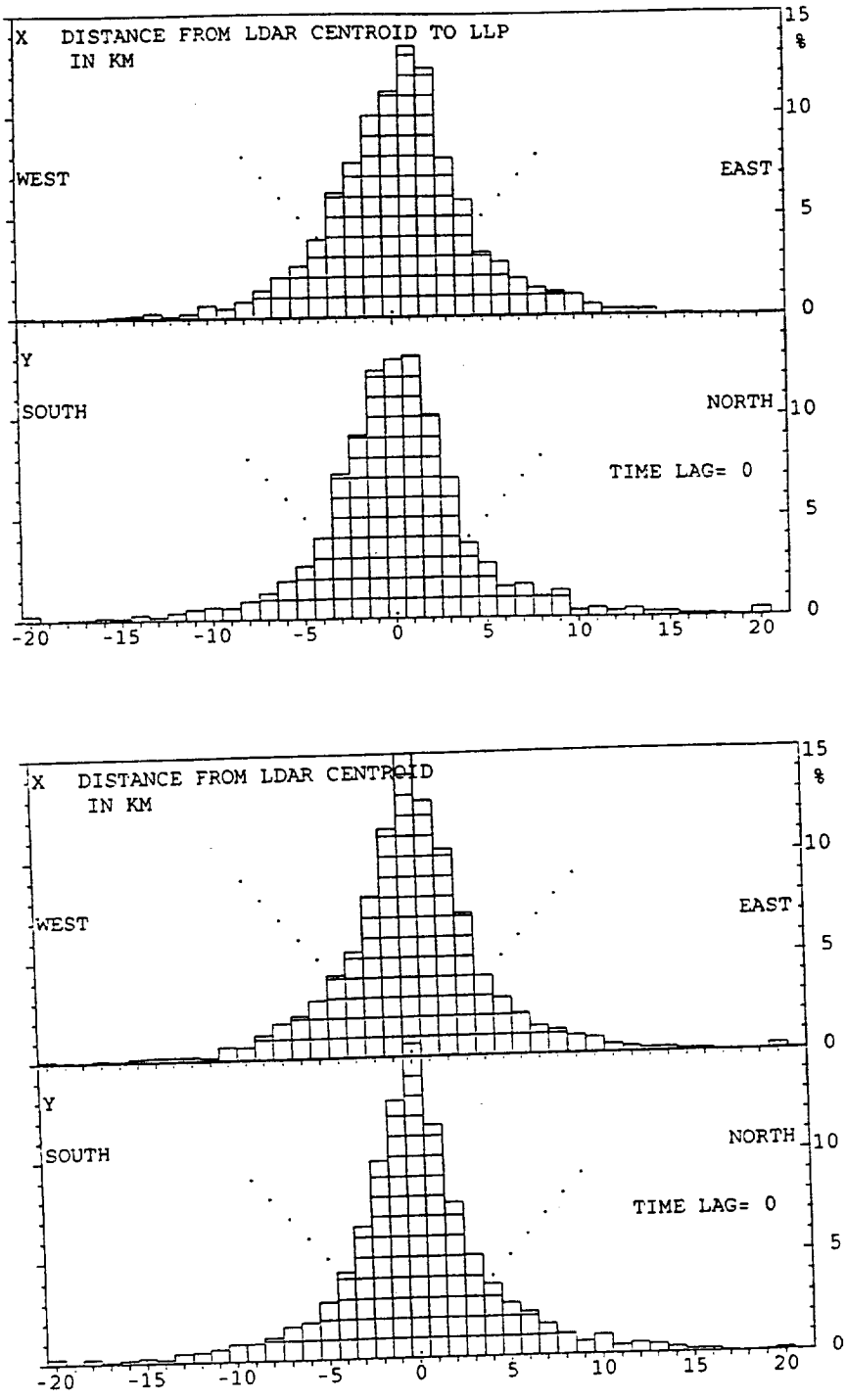

Figure 3-3. Locations of ground strikes relative to LDAR storm center, by distance east/west and north south. a. (Top) LLP ground strikes. b. (Bottom) LDAR-derived ground strikes, using LDAR data cubes below 2.5 km.

probably spurious. There were 2483 moving LDAR storm-minutes at time 0, decreasing to 1553 by time = 20 minutes. Compositing is in an LDAR storm-relative frame of reference for "Moving" storms.

The values in Table 3-2 indicate that there is about a 1% increase in percentages at time 0 for quasi-stationary and moving storms. This is because a few storms have been discarded for which no LDAR storm velocity could be determined. These tended to be short-lived storms, probably of dubious validity.

TABLE 3-2. COMPOSITING OF FUTURE GROUND STRIKES WITH RESPECT TO THE CURRENT LDAR STORM BOUNDARIES, BY CATEGORIES OF STORM MOVEMENT, IN PERCENT

TIME	ALL STORMS			QUASI-STAT.			MOVING		
	in	<1	<2	in	<1	<2	in	<1	<2
0	85	97	98	86	98	99	86	97	99
1	75	86	90	80	89	93	77	87	90
3	71	84	88	79	88	93	74	84	89
5	64	77	84	71	81	86	67	79	84
10	44	59	67	51	65	68	50	61	67
15	31	42	50	41	54	63	36	47	53
20	20	29	35	30	41	50	26	36	39

Notes: "in" means inside LDAR storm boundaries
<1 means within 1 km beyond LDAR storm edge
<2 means within 2 km beyond LDAR storm edge

The values in Table 3-2 seem to indicate the merit of using compiling according to LDAR storm movement. Percentages under "All Storms" are with respect to the initial position of the LDAR storm while, in reality, more than 75% of the storms were moving. Partly for this reason, the percentage of future ground strikes falling inside the current LDAR storm position decreases to 20% by 20 minutes. For storms that truly were quasi-stationary, the percentage is 30% at 20 minutes, a 10% "improvement", and is 50% versus 35% for ground strikes within 2 km beyond LDAR storm edge. Increases of up to 6% are seen in the percentage of ground strikes inside the LDAR storm due to use of the LDAR storm-relative frame of reference with moving storms. The increase is smaller for ground strikes within 2 km beyond storm edge.

One way to summarize Table 3-2 is to note that more than half of the ground strikes occur outside the boundaries of the current LDAR storm after 10 minutes. Half of the ground strikes occur more than 2 km beyond the boundaries of the current LDAR storm after 20 minutes for quasi-stationary storms, and after 15 minutes for moving storms.

The probable explanation of the increase in percentage of ground strikes occurring outside the LDAR storm with time is that thunderstorms and their lightning ground strike patterns evolve on rather short time scales. Thunderstorms and their lightning patterns tend to grow with time, and that growth has not been anticipated or factored into the compositings of Table 3-2. Some of the "external" ground strikes of Table 3-2 are also due to the development of new storms along the flanks of the existing storm.

The data base can be used to determine if future ground strikes occur preferentially on one flank of the the LDAR storm. Figure 3-4 shows the composite locations of ground strikes after 10 minutes, with respect to quasi-stationary storms (Fig. 3-4a) and with respect to moving storms in a storm-relative frame of reference (Fig. 3-4b). There is a slight preference for future ground strikes on the south and east flanks of the current quasi-stationary LDAR storms. There is a slight preference for future ground strikes on the rear flank of moving LDAR storms. In the mean the rear flank was the west-southwest flank in this study, though there was much variation in direction of storm movement.

3.6 PROBABILITY OF GROUND STRIKES MORE THAN 5 NAUTICAL MILES BEYOND LDAR STORM EDGE

Weather forecasters must issue lightning advisories when lightning is anticipated within 5 nautical miles (9.25 km) of a warning area. Table 3-3 shows the frequency of LLP ground strikes that occur more than 5 n.mi. beyond the edge of the LDAR storm boundary. In the case of moving storms at future times, the position is relative to the projected position of the current LDAR storm boundaries. Probabilities for "All Storms" and "Quasi-Stationary" storms are with respect to the current positions of the LDAR storm boundaries.

TABLE 3-3. PROBABILITY OF GROUND STRIKES MORE THAN 5 N.MI. BEYOND EDGE OF LDAR STORM

TIME	ALL STORMS	QUASI-STAT.	MOVING
0	0.5%	0.0%	0.4%
1	3.0	2.5	2.7
3	2.6	2.3	2.5
5	3.4	4.0	3.7
10	7.5	8.5	7.3
15	14.8	7.9	15.5
20	30.0	16.1	30.8

The probabilities shown in Table 3-3 are not point probabilities, but apply to large areas. A conservative estimate of the probability that a particular area of size 1 km^2 will be struck can be obtained from the values in Table 3-3 by dividing by 61.3. This factor has been derived by using a mean LDAR storm edge position 7.64 km from the LDAR storm center, and very conservatively assuming that all ground strikes occurred between 9.25 and 10.25 km beyond LDAR storm edge. Thus, the probability of a particular square kilometer area being hit when beyond 5 n.mi. from the LDAR storm edge is less than 0.008% during the current minute and not more than 0.5% after 20 minutes. Depending upon what risk is acceptable, forecasters can probably make effective use of the current LDAR storm boundary (and not need to add an extra margin beyond it) in issuing advisories for lightning within a 5 n.mi. radius of warning sites.

3.7 CESSATION OF LDAR ACTIVITY AND END OF GROUND STRIKE THREAT

Weather forecasters must issue statements indicating that the threat of ground strikes has ceased. One potential tool in this task is the disappearance of the LDAR storm. However, some LDAR storms are intermittent--especially in their late stages--and may reappear after being inactive for a few minutes. Do these storms still pose a ground strike threat? Table 3-4 indicates the probability of an LDAR storm still yielding a ground strike after being inactive (producing no LDAR events) for the indicated number of minutes.

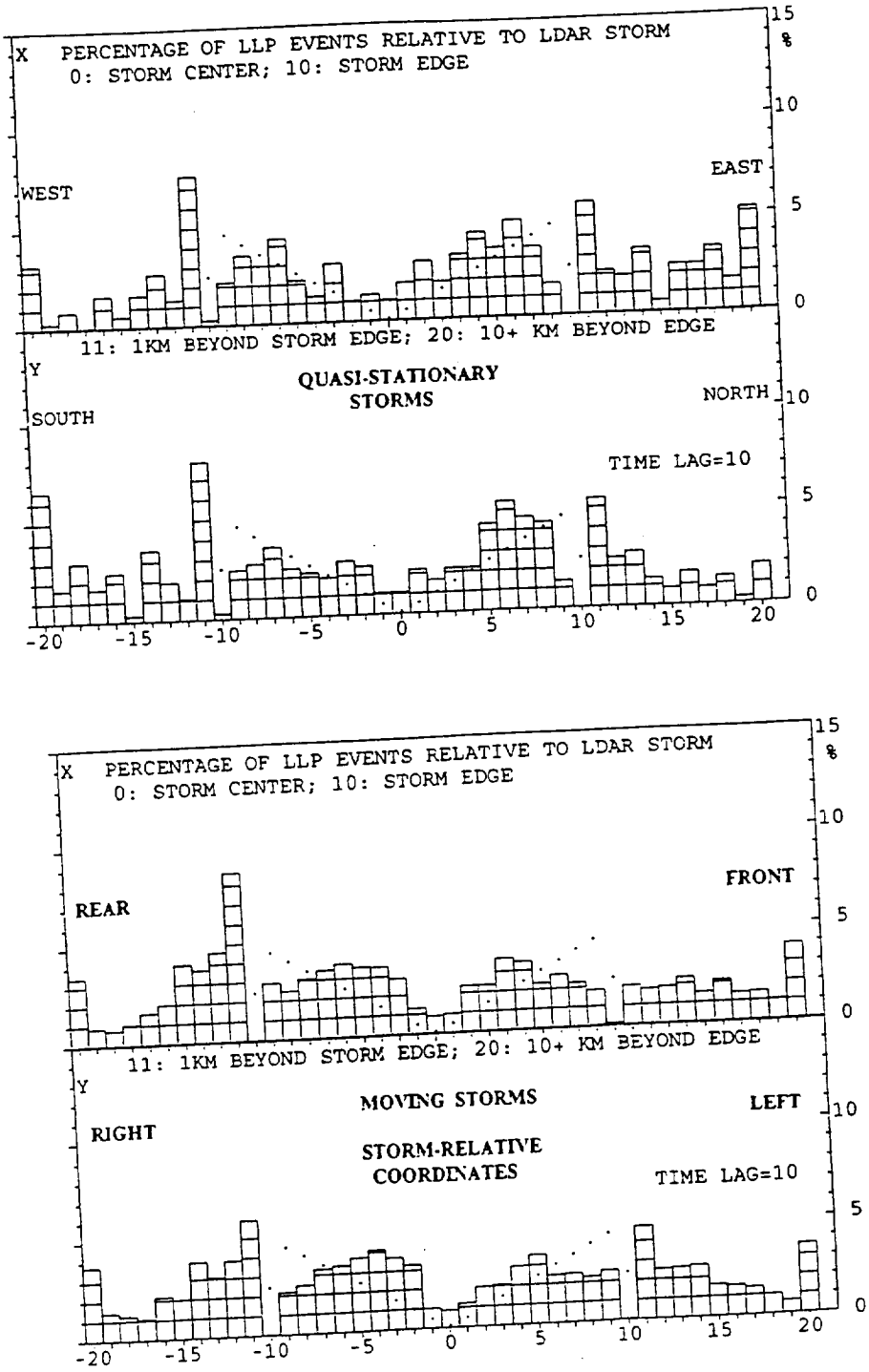

Figure 3-4. Locations of ground strikes 10 minutes later, relative to current LDAR storm center, by fractional positions east/west and north/south.
a. (TOP) Quasi-stationary storms; compositing relative to current position.
b. (Bottom) Moving storms; compositing relative to projected position of current LDAR storm after 10 minutes, in storm-relative coordinates.

TABLE 3.4 PROBABILITY OF AN LDAR STORM THAT HAS BEEN INACTIVE YIELDING A FUTURE GROUND STRIKE, AS A FUNCTION OF THE PERIOD OF INACTIVITY

INACTIVE PERIOD	PROBABILITY
1 min	46%
> 1	22
> 2	13
> 3	7
> 4	5
> 5	3
> 6	2
> 7	1
> 8	0.5

3.8 DIFFERENCES BETWEEN STORMS THAT PRODUCE GROUND STRIKES AND THOSE THAT NEVER PRODUCE GROUND STRIKES

LDAR storms that never produced ground strikes had short duration. Eighty-nine percent had duration of 5 minutes or less. Only 27% of the LDAR storms which produced LLP ground strikes had durations that brief. Many (55%) of the LDAR storms which never produced ground strikes were 1-minute events, representing odd discharge patterns into areas not previously affected. This caused an appreciable (> 6 km), momentary shift in storm centroid and caused the objective storm classification scheme to trigger a new storm identification number. During the next minute, when the odd discharge was no longer present, the LDAR storm centroid returned to near its previous location, and the previous storm identification number was resumed.

Only 10% of the LDAR storms having 1 or 2-minute duration were associated with LLP ground strikes. Only 6% of the LDAR storms having 1 or 2-minute duration were associated with LLP ground strikes if they contained less than 100 LDAR events per minute. From a weather forecasting perspective, the implication is that sudden large bursts of low-density LDAR activity that extend beyond the previous LDAR storm boundary do not normally pose a ground strike threat.

The maximum number of LDAR events is less in LDAR storms that never produce an LLP ground strike. Sixty-two percent of such storms never contained more than 50 LDAR events per minute. Only 11% of the LDAR storms associated at some time with LLP ground strikes peaked at such a low LDAR data rate. By contrast, 81% of the LDAR storms associated with LLP ground strikes contained more than 150 LDAR events per minute at some point during their existence.

3.9 LDAR STORM DIFFERENCES DURING MINUTES WITH AND WITHOUT GROUND STRIKES

It was indicated previously that only 41% of the LDAR storm minutes are associated with LLP ground strikes. Is the LDAR storm character different during minutes with LLP ground strikes? For brevity of wording, LDAR storm minutes associated with LLP ground strikes will be referred to below as "LLP minutes"; those without ground strikes will be referred to as "non-LLP minutes".

LLP minutes had many more LDAR events per storm. The median values were 500 for LLP minutes and 165 for non-LLP minutes. Of course, some of these LDAR events could be produced by the ground strike itself.

LLP minutes had a much bigger LDAR storm volume. The median values were 200 km^3 for LLP minutes and 50 km^3 for non-LLP minutes. Again, some of this difference could be due to an expansion of LDAR storm volume due to the ground strike extending the storm volume downward to the surface. However, this hypothesis is

not fully supported by LDAR storm height data. There was little difference in the median heights of the LDAR storm centroid during LLP and non-LLP minutes. Likewise, there was little difference in the median Z95 heights, suggesting that LDAR storm top was not significantly different (at least with the vertical resolution used in this study). LLP minutes, however, did have larger storm depth, as measured by standard deviation of z. Using twice the standard deviation, median values were 4.15 versus 2.75 km for LLP and non-LLP minutes, respectively. Some downward extension of the LDAR storm may be revealed here.

LLP minutes had larger LDAR storm cross-sectional area. The median values were 80 km^2 for LLP minutes and 36 km^2 for non-LLP minutes.

Despite having larger LDAR storm volume and cross-sectional areas, LLP-minutes also had larger LDAR volume densities and LDAR area densities than non-LLP minutes. Median values for LDAR volume density were 3.1 and 2.2 LDAR events per km^3, respectively. Median values for LDAR area density were 6.6 and 3.7 LDAR events per km^2, respectively.

3.10 LDAR-BASED PARAMETERS IN RELATION TO VARIATIONS IN GROUND STRIKE RATE

Because section 3.9 showed many differences between LDAR storm characteristics during minutes with and without LLP ground strikes, and because some storms (such as in Fig. 2-7) revealed that LDAR-derived parameters were correlated to number of LLP ground strikes, the correlation between LDAR-derived storm parameters and ground strike rate was examined in more detail. Temporal variations of eight LDAR-derived parameters were examined in relation to temporal variations in numbers of LLP ground strikes associated with the LDAR storms. LDAR storms were only included in these correlation studies if they were associated with LLP ground strikes at some time during their existence. The eight LDAR-derived storm parameters examined were: (1) NLDAR, number of LDAR data points within the LDAR storm volume; (2) VOL, LDAR storm volume; (3) AREA, LDAR storm area; (4) VOLDENS, LDAR volume density; (5) AREADENS, LDAR area density; (6) ZMEAN, LDAR storm centroid height; (7) ZSD, standard deviation of height of LDAR cubes within the LDAR storm volume, a measure of LDAR storm depth; (8) Z95, the height below which 95% of the LDAR data occurs within the LDAR storm.

Table 3-5 shows correlations between number of LLP ground strikes per minute associated with the LDAR storm and LDAR storm parameter values. The correlations are tabulated for simultaneous relationships (time lag 0), and for LLP ground strikes which lag the LDAR storm parameter values by the indicated numbers of minutes. The five LDAR-derived parameters with highest correlations are listed for each time lag, in order of decreasing correlation.

In the correlation studies, ZSD, a measure of LDAR storm depth, had the highest correlation for 9 of the 11 lag times. LDAR storm volume had the highest correlation for the other two lag times, 1 and 5 minutes. The number of LDAR data points within the LDAR storm had the third best correlation overall, having the second highest correlation for 3 lag times. Mean LDAR Storm height ranked second for 2 lag times. Z95 and LDAR storm area each had third highest correlation for some lag time. Despite impressive relationships for some storms, LDAR volume and area densities never ranked better than sixth for any lag time when all LDAR storms that produced LLP ground strikes were considered.

Unfortunately, the correlations in Table 3-5 were highest for time lag of zero and generally decreased with increasing lag time. The exception was for lag time of two minutes, when the correlation was higher than at 1 minute. Probably the contribution of LDAR data points to the LDAR storm characteristics by the ground strike itself is causing the highest correlation for lag time of zero.

It must also be noted that even the highest correlation by an individual LDAR storm parameter is 0.592. This means that variations in LDAR storm depth from minute to minute would explain only 35% of the variations in number of LLP ground

TABLE 3-5. CORRELATION BETWEEN LDAR-DERIVED STORM PARAMETERS AND LLP GROUND STRIKE RATE, AS A FUNCTION OF LAG TIME BETWEEN LDAR PARAMETER AND LLP GROUND STRIKE

LAG	RANK 1	RANK 2	RANK 3	RANK 4	RANK 5
0	ZSD 0.592	VOL 0.579	AREA 0.542	NLDAR 0.521	ZMEAN 0.495
1	VOL 0.492	ZSD 0.492	NLDAR 0.457	AREA 0.441	ZMEAN 0.422
2	ZSD 0.497	VOL 0.486	NLDAR 0.460	AREA 0.441	ZMEAN 0.439
3	ZSD 0.478	VOL 0.466	NLDAR 0.446	ZMEAN 0.433	AREA 0.424
4	ZSD 0.450	VOL 0.433	ZMEAN 0.415	NLDAR 0.414	AREA 0.396
5	VOL 0.433	ZSD 0.429	NLDAR 0.422	ZMEAN 0.402	AREA 0.392
6	ZSD 0.396	NLDAR 0.384	VOL 0.383	ZMEAN 0.377	Z95 0.359
7	ZSD 0.376	ZMEAN 0.361	Z95 0.345	VOL 0.344	NLDAR 0.344
8	ZSD 0.355	NLDAR 0.348	VOL 0.347	ZMEAN 0.340	Z95 0.325
9	ZSD 0.337	NLDAR 0.323	VOL 0.321	ZMEAN 0.315	Z95 0.303
10	ZSD 0.300	ZMEAN 0.291	Z95 0.278	NLDAR 0.265	VOL 0.259

NOTE: LAG is LLP ground strike time minus LDAR storm parameter time, in minutes

strikes per minute using a regression approach. However, experience with multiple linear regression shows that this would be a good start if additional LDAR storm parameters were not highly intercorrelated. If the temporal variations of other LDAR storm parameters were poorly correlated to ZSD variations, then they would make additional contributions in a multiple regression equation aimed at explaining the variations in number of LLP ground strikes per minute from LDAR storms. Time has not permitted further pursuit of this topic.

IV. CONCLUDING REMARKS

The ultimate goal of this study has been to begin a process that may help operational weather forecasters give better and more timely lightning advisories. LDAR seems to provide information that can be useful to the forecasters.

In section I, five questions were posed that operational weather forecasters might ask regarding use of the LDAR data. The answers to those questions are reviewed here.

What is the lead time between the first detection of LDAR events and ground strikes? The average lead time is 5.26 minutes. Only 11% of the LDAR storms produced LLP ground strikes during the first minute of their existence (Section 3.1).

Are there preferred locations of occurrence of ground strikes relative to the pattern of discharges detected by LDAR? Eighty-five percent of the LLP ground strikes occur within the boundaries of the LDAR-defined storm, and 98% occur either within the LDAR storm boundaries or within 2 km beyond them. The highest concentration of ground strikes occurs near the center of the LDAR storm (Section 3.4).

Can future positions of ground strikes be anticipated through knowledge of the current LDAR event pattern? The percentage of ground strikes falling within the boundaries of the current LDAR storms decreases with time. Half of the ground strikes occur more than 2 km beyond the boundaries of the current LDAR storm (in the case of quasi-stationary storms) or the projected position of the current LDAR storm (in the case of moving storms) after 15 minutes for moving storms and after 20 minutes for quasi-stationary storms. There was some preference for future ground strikes to occur on the south and east flanks of quasi-stationary storms and on the rear (west-southwest) flank of moving storms in this study (Sections 3.5, 3.6).

Are there signatures in the LDAR data that can be used to determine when the threat of ground strikes has ended? In latter stages of LDAR storms, they often become intermittent, often disappearing for several minutes on the LDAR display. Only 5% of LDAR storms have future ground strike if they have disappeared for more than 4 minutes; only 0.5% if they have disappeared for more than 8 minutes (Section 3.7). Other signatures probably exist, but have not been quantified.

Are there signatures in the LDAR data that reveal which storms produce ground strikes and which do not? Sudden large bursts of low-density LDAR activity that extend beyond the previous LDAR storm boundary do not normally pose a ground strike threat. There are a number of LDAR-derived parameters that show significant differences, on average, between storms that produce ground strikes and those that do not (Sections 3.8-3.10). Further research is needed before these parameters can be used reliably.

LDAR shows great promise as a tool for better understanding the dynamics of thunderstorm electrification processes, especially when the LDAR data is used in conjunction with Doppler radar, surface mesonet, and wind profiler network data that can reveal the location of convergence zones. These convergence zones, when related to the flanks of LDAR- and radar-defined storms, can suggest the preferred flanks upon which new thunderstorm cell growth will be preferred and where future ground strikes may be concentrated. Intercomparison of field mill data should also prove informative. Expert system and neural network studies of lightning prediction may be ways to assimilate the various types of information.

REFERENCES

1. Maier, M.W., A.G. Boulanger, and R.I. Sax: An initial assessment of flash density and peak current characteristics of lightning flashes to ground in South Florida. NUREG/CR-1024, U.S. Nuclear Regulatory Commission, 1979.

2. MacGorman, D.R., M.W. Maier, W.D. Rust: Lightning strike density for the contiguous United States from thunderstorm duration records. NUREG/CR-3759, U.S. Nuclear Regulatory Commission, 1984.

3. Maier, L.M., E.P. Krider, and M.W. Maier: Average diurnal variation of summer lightning over the Florida Peninsula. *Mon. Weather Rev., 112*(6), June, 1984, pp. 1134-40.

4. Orville, R.E., R.W. Henderson, and L.F. Bosart: An East Coast lightning detection network. *Bull. Amer. Meteorological Soc., 64*, 1983, pp. 1029-37.

5. Krider, E.P., A.E. Pifer and D.L. Vance: Lightning direction-finding system for forest fire detection. *Bull. Amer. Meteorological Soc., 61*, 1980, pp. 980-86.

6. Lennon, C. and L. Maier: Lightning mapping system. NASA CP-3106, Vol, II, 1991 International Aerospace and Ground Conference on Lightning and Static Electricity, 1991, pp. 89-1 to 89-10.